Electronic Supplementary Material (ESI) for ChemComm.

Supplementary Information

Modulation of ΔE_{ST} and room temperature phosphorescence in carbazole derivatives

Komal Vasant Barhate[a], Amey P. Wadawale[b], K. R. S. Chandrakumar[c]* and Neeraj Agarwal[a]*

[a]*School of Chemical Sciences, UM DAE Centre for Excellence in Basic Sciences, University of Mumbai, Kalina, Santacruz (E), Mumbai 400098, India*

[b]*Chemistry Division, Bhabha Atomic Research Center, Mumbai 400085, India*

[c]*Theoretical Chemistry Section, Bhabha Atomic Research Centre, Trombay,Mumbai 400085, India*

Contents:

Materials and Methods:

All solvents and chemicals were obtained from Sigma-Aldrich and SD Fine Chemicals, India, and used as received. Silica gel (100–200 mesh) was used for column chromatographic separation. A Bruker Avance 400 MHz spectrometer was used to obtain ^{1}H NMR, ^{19}F NMR, & ^{13}C NMR spectra. Tetramethylsilane was used as an internal reference, and the residual proton in $CDCl_3$ (δ = 7.26 ppm) & $C_2D_2Cl_4$ (δ = 6 ppm) was used as a reference peak. A Bruker MALDI-TOF and Agilent HRMS spectrometers were used for mass spectra. Shimadzu 1800, and HORIBA FluoroMax-4 spectrometers were used to collect the absorption and emission spectra, respectively. A HORIBA Deltaflex nano-LED-based time-correlated single-photon counting (TCSPC) spectrometer with 290 nm Nano led as an excitation source was used for fluorescence decay studies in solution. Emission decay profiles in powder at 298 K were recorded using 395 nm spectra led as an excitation source and the data were collected at the magic angle (54.7°). Monitoring the scattered excitation light from SiO_2 particles suspended in water gave us the instrument response function (IRF). The IRF was found to be ∼100 ps. Emission and lifetimes at cryogenic temperature were recorded on FLS1000 fluorescence spectrophotometer equipped with a xenon arc lamp (Xe900) and a microsecond flash-lamp (μF900). X-ray crystallography was achieved on XtaLAB Synergy, Dualflex, HyPix four-circle diffractometer with a micro-focus sealed X-ray tube using a mirror as monochromator and a HyPix detector using Cu Kα radiation (λ = 1.54184 Å) from a single crystal at 298 K The luminescent photos and videos were taken by iPhone 13 under ambient conditions. The density functional theory (DFT) based calculations were done using the ORCA-based electronic structural program. The optimization and frequency calculations were performed using the BP86 exchange-correlation function with the double-ζ valence plus polarization function (DZVP) basis set basis set, with a D3(BJ) empirical dispersion correction.

Synthesis:

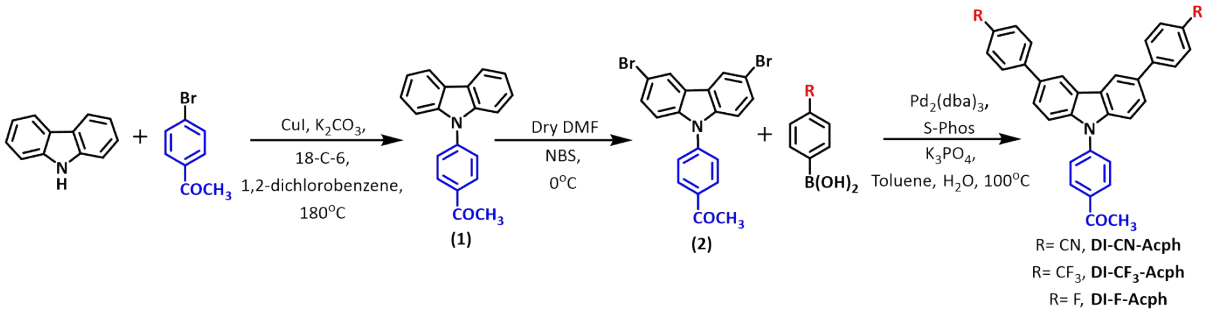

Scheme S1: Schematic representation of the synthesis of N-substituted carbazole derivatives

1-(4-(9H-carbazol-9-yl) phenyl) ethan-1-one **(1)** was synthesized as given in ref.[1]

1-(4-(3,6-dibromo-9H-carbazol-9-yl) phenyl) ethenone **(2):** 1-(4-(9H-carbazol-9-yl) phenyl) ethanone (0.710 g, 2.18 mmol) was dissolved in dimethylformamide (DMF) (10 mL) in a 100 mL round bottom flask. After the solution was cooled at 0°C, a solution of N-bromosuccinimide (NBS) (0.88 g, 4.97 mmol) in DMF (2 mL) was added dropwise. The reaction mixture was allowed to warm to room temperature and stirred for 2h in the absence of light. The mixture was then poured into cold water (250 mL), white precipitate obtained by filtration was purified by column chromatography using dichloromethane/hexane (1:9) to get pure 1-(4-(3,6-dibromo-9H-carbazol-9-yl) phenyl) ethenone **(2)** as white crystals (1.03 g, 92 %).[2]

General procedure for the synthesis of DI-R-Acph derivatives:

1-(4-(3,6-dibromo-9H-carbazol-9-yl) phenyl) ethenone **(2)** (0.05 g, 0.11 mmol), boronic acid (3 equi.), anhydrous K_3PO_4 (0.072 g, 0.34 mmol), $Pd_2(dba)_3$ (0.01 g, 10 mol %), S-Phos (0.008 g, 20 mol %), were placed in an oven-dried Schlenk tube and capped with a rubber septum and then evacuated. A mixture of 3 mL toluene and 0.5 mL water was added via syringe and then again evacuated and refilled with argon (the sequence was repeated three times). The reaction was carried out at 100 ^{0}C for 18 h and was monitored by the TLC method. On completion of the reaction, the reaction mixture was cooled down to room temperature and water was added. The water layer was washed with dichloromethane three times. Further organic layer was washed with brine solution and dries over anhydrous Na_2SO_4. The solvent

was evaporated by rotatory evaporator and the crude product was further purified by column chromatography with dichloromethane/hexane (1:4) as eluent.

(i) 4, 4'-(9-(4-acetylphenyl)-9H-carbazole-3,6-diyl) di benzonitrile (**DI-CN-Acph**): Yield 38 mg (68%);M.P.: above 250 °C; ^{1}H NMR (400 MHz, $C_2D_2Cl_4$): *δ ppm* 8.49 (s, 2H), 8.30 (d, 2H,), 7.90 (d, 4H), 7.85 (t, 6H), 7.78 (d, 2H), 7.66 (d, 2H, *J* = 6.4 Hz), 2.73 (s, 3H); ^{13}C NMR (100 MHz, $C_2D_2Cl_4$): *δ ppm* 197.30, 146.02, 141.35, 141.03, 136.20, 132.86, 132.37, 130.52, 127.93, 126.58, 126.32, 124.45, 119.51, 110.96, 110.24, 26.98; IR: ν (cm^{-1}) 2342, 2216, 1681, 1595, 1460, 1368, 1235, 1172, 1107, 912, 842, 750, 646, 560; HR-MS: Calcd. For $C_{34}H_{21}N_3O$ 487.1685; obsd. 522.1369 $(M+Cl)^+$

(ii) 1-(4-(3,6-bis(4-(trifluoromethyl)phenyl)-9H-carbazol-9-yl)phenyl)ethan-1-one (**DI-CF_3-Acph**): Yield 35 mg (54%); M.P.: above 250 °C; ^{1}H-NMR (400 MHz, $CDCl_3$): *δ ppm* 8.45 (s, 2H), 8.30 (d, 2H, *J* = 8 Hz), 7.87 (d, 4H, *J* = 8 Hz), 7.78 (d, 6H, *J* = 8 Hz Hz), 7.73 (s, 2H), 7.61 (d, 2H, *J* = 8.4 Hz), 2.76 (s, 3H); ^{13}C-NMR (100 MHz, $CDCl_3$): *δ ppm* 196.91, 145.03, 141.62, 140.66, 135.98, 132.90, 130.33, 129.08, 128.75, 127.49, 126.47, 126.11, 125.84, 125.80, 125.77, 124.44, 123.06, 119.30, 110.54, 26.74; ^{19}F NMR ():*δ ppm* -62.26; IR: ν (cm^{-1}) 1681, 1595, 1476, 1326, 1273, 1107, 1068, 1007, 955, 794, 655, 585; MALDI-TOF mass calcd. For $C_{34}H_{21}F_6NO$ (573.53); obsd. 573.21 $(M)^+$

(iii) 1-(4-(3,6-bis(4-fluorophenyl)-9H-carbazol-9-yl)phenyl)ethan-1-one **(DI-F-Acph**): Yield 40 mg (74%); M.P.: above 250°C; ^{1}H-NMR ($CDCl_3$, 400 MHz, δ ppm): 8.36 (s, 2H), 8.28 (d, 2H, *J* = 8.4 Hz), 7.79 (d, 2H, *J* = 8.4 Hz), 7.71 (d, 4H, *J* = 8 Hz Hz), 7.68 (d, 2H, *J* = 10 Hz), 7.58 (d, 2H, *J* = 8.4 Hz), 7.20 (t, 4H, *J* = 8.4 Hz, *J* = 8.4 Hz), 2.75 (s, 2H); ^{13}C-NMR (100 MHz, $CDCl_3$): *δ ppm* 196.95, 163.48, 161.03, 141.95, 140.05, 137.76, 137.73, 135.69, 133.43, 130.27, 128.83, 128.75, 126.34, 125.84, 124.44, 118.88, 115.80, 115.59, 110.27, 26.73; ^{19}F NMR ():*δ ppm* -116.48; IR: ν (cm^{-1}) 1683, 1595, 1471, 1361, 1220, 1161, 952, 833, 771, 586, 520; MALDI-TOF mass calcd. For $C_{32}H_{21}F_2NO$ (473.52); obsd. 472.52 $(M)^+$

Characterization:

(i) By NMR spectroscopy

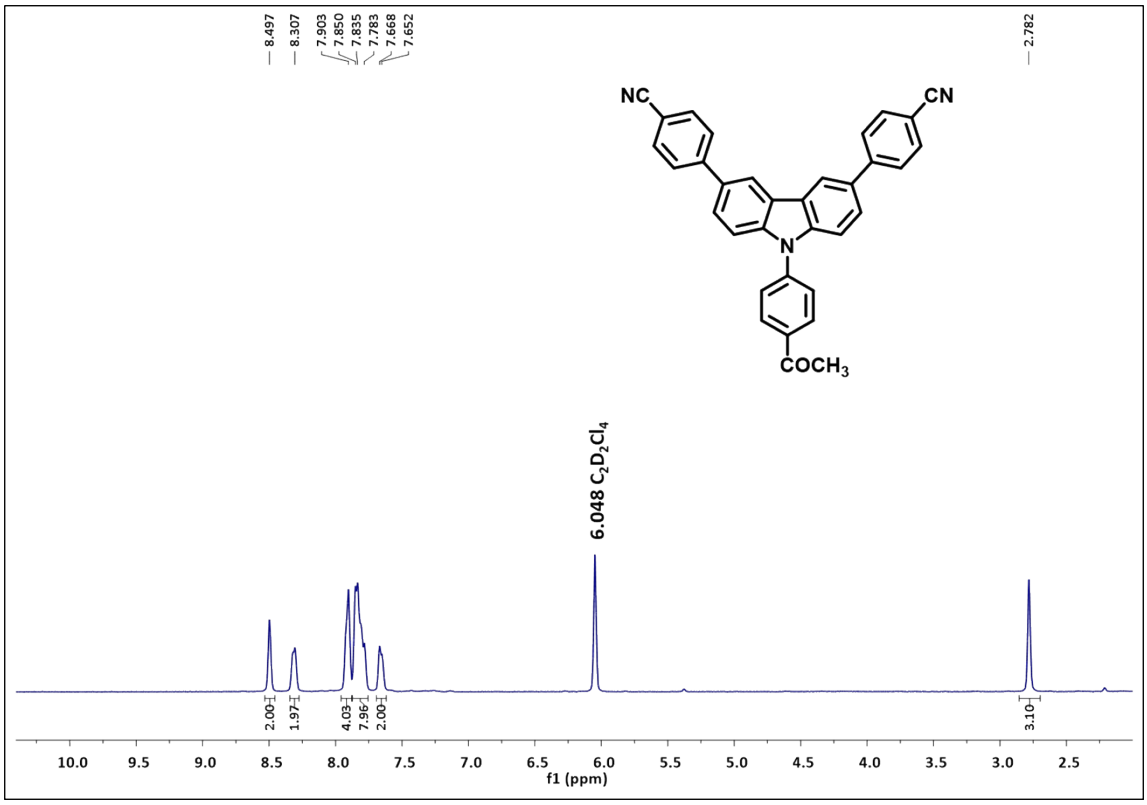

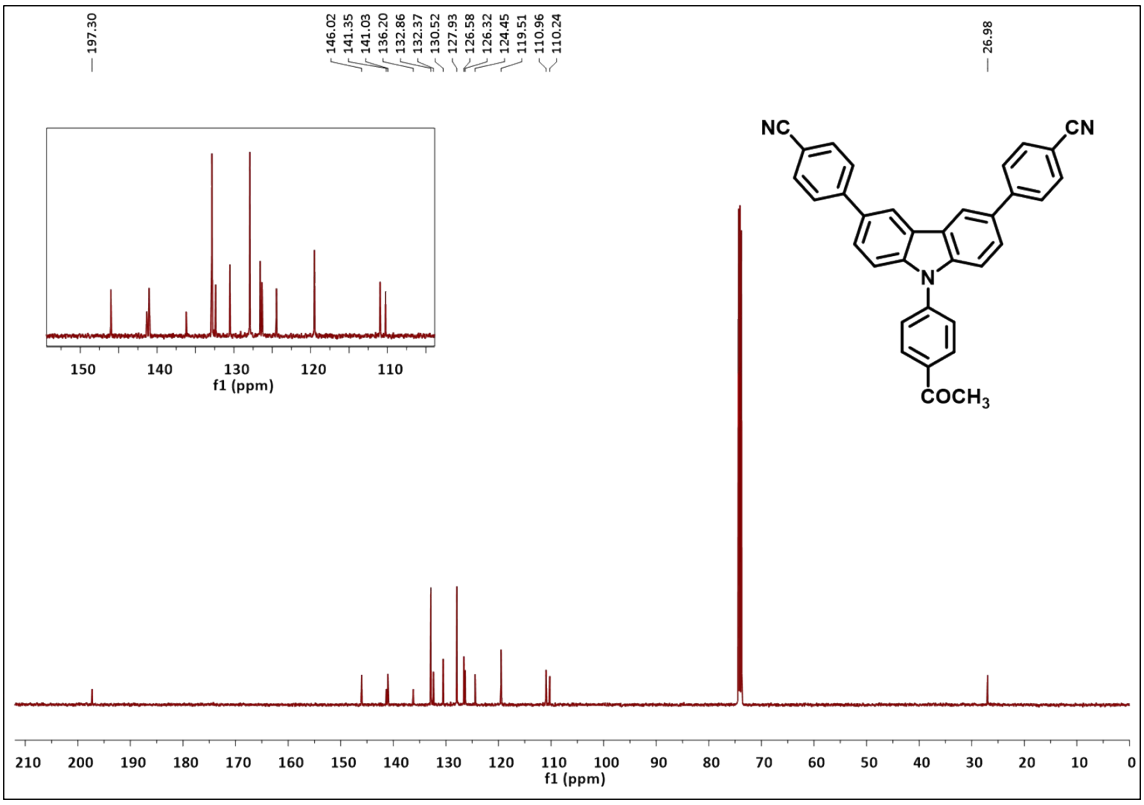

Figure SI 1: ^{1}H NMR (top) and ^{13}C NMR (bottom) spectra of **DI-CN-Acph** in $C_2D_2Cl_4$

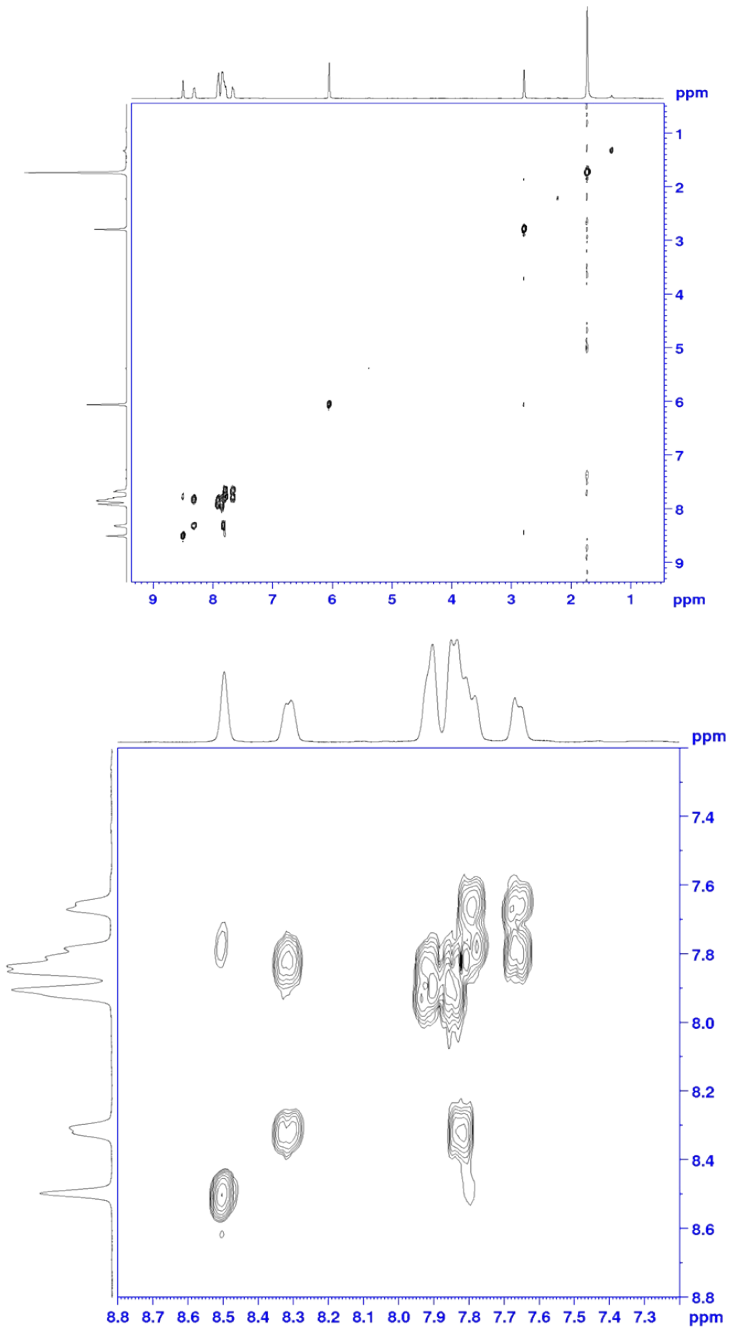

Figure SI 2: COSY spectrum of **DI-CN-Acph** in $C_2D_2Cl_4$. Top: Full spectrum and Bottom: Aromatic region

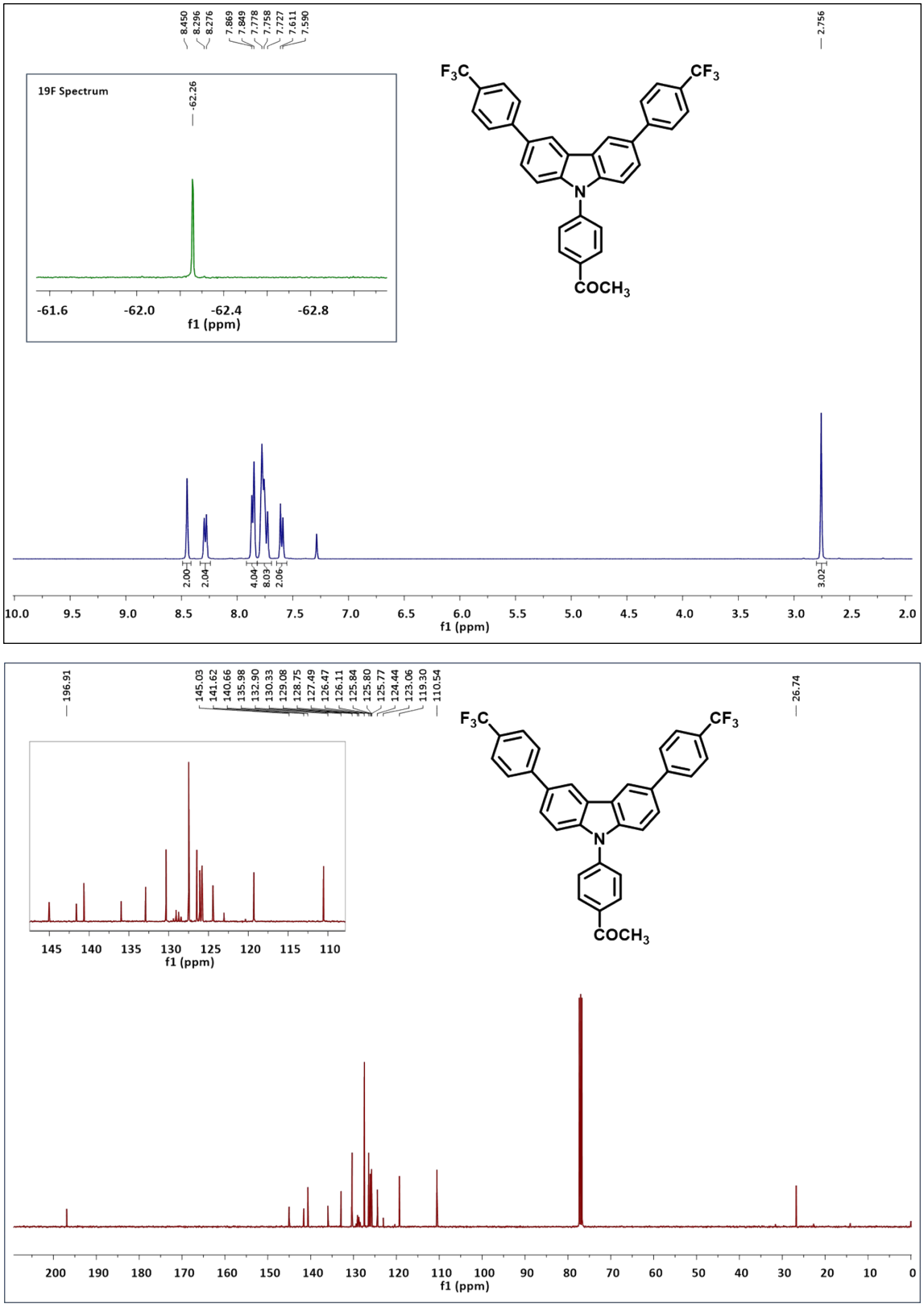

Figure SI 3: ^{1}H NMR & ^{19}F (top, inset) and ^{13}C NMR (bottom) spectra of **DI-CF_3-Acph** in $CDCl_3$

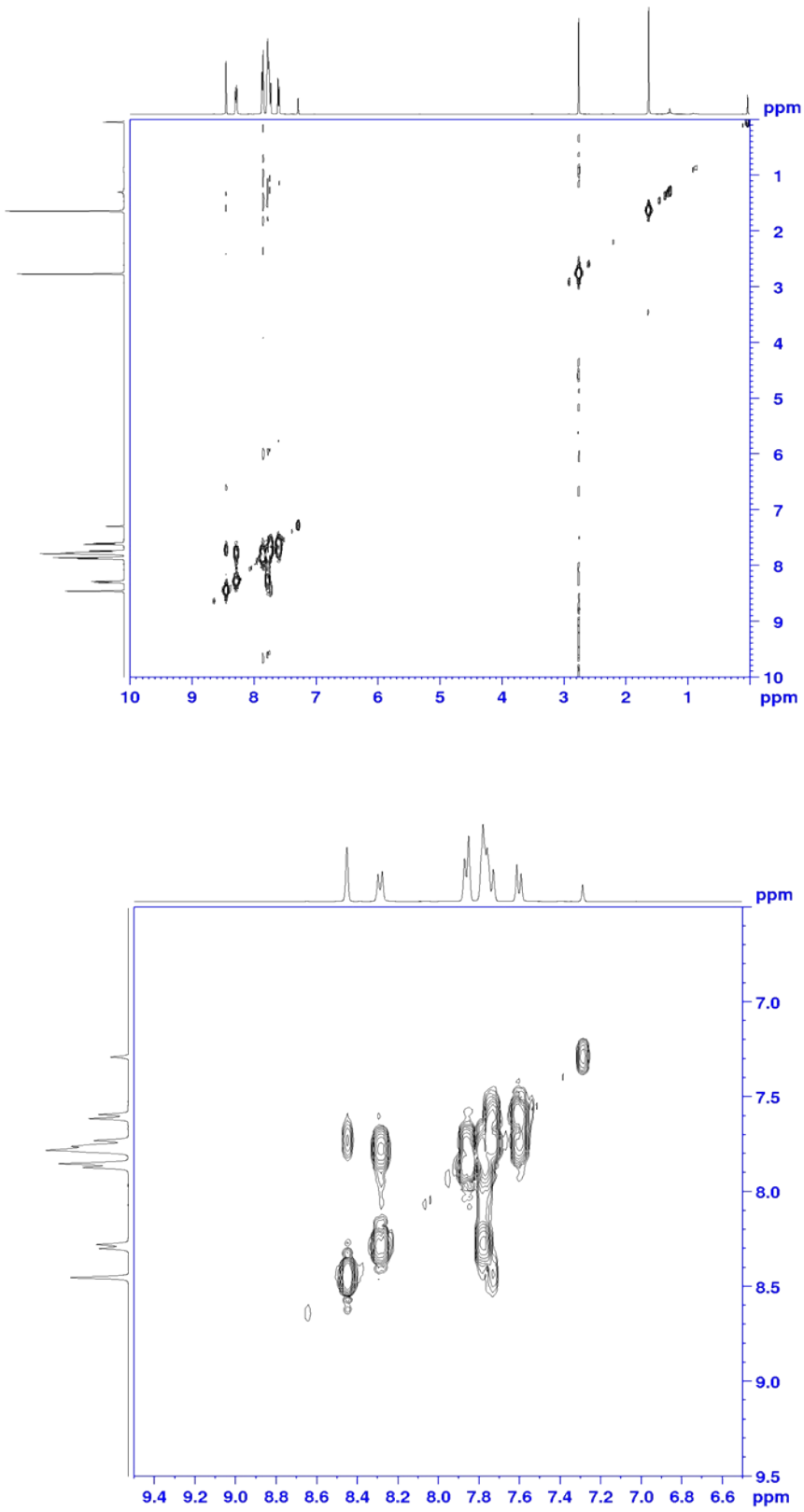

Figure SI 4: COSY spectrum of **DI-CF_3-Acph** in $CDCl_3$. Top: Full spectrum and Bottom: Aromatic region

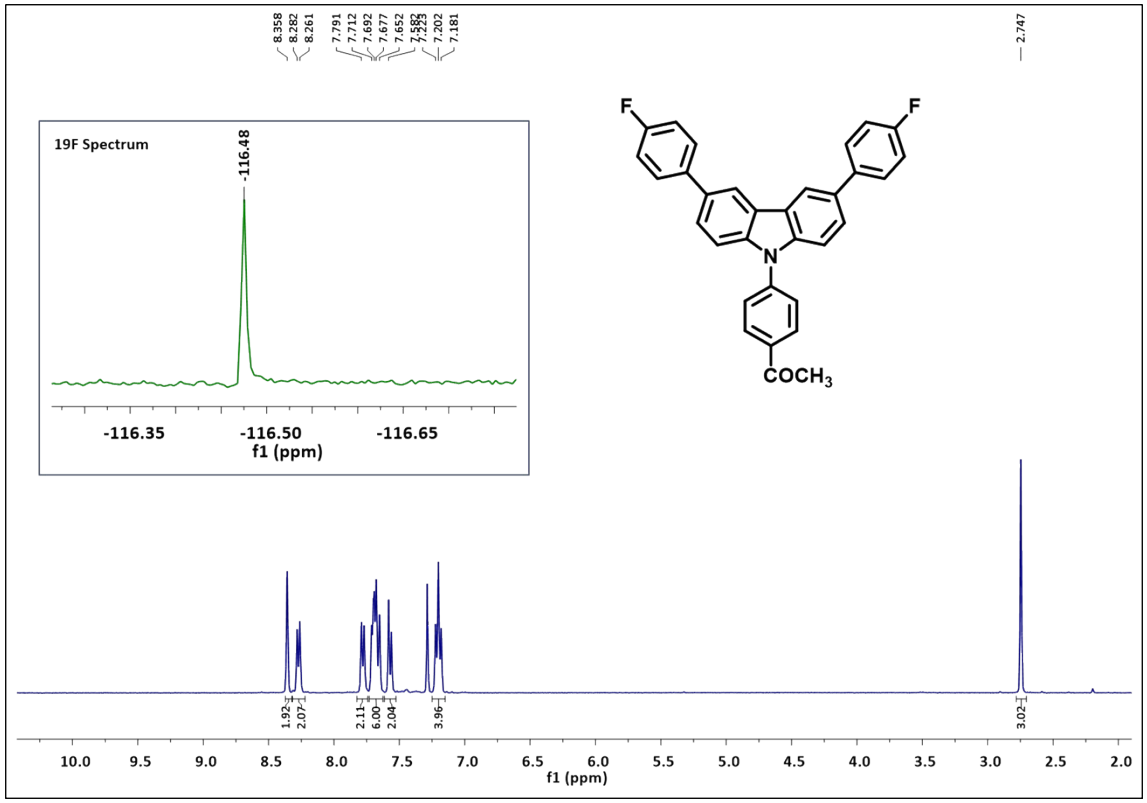

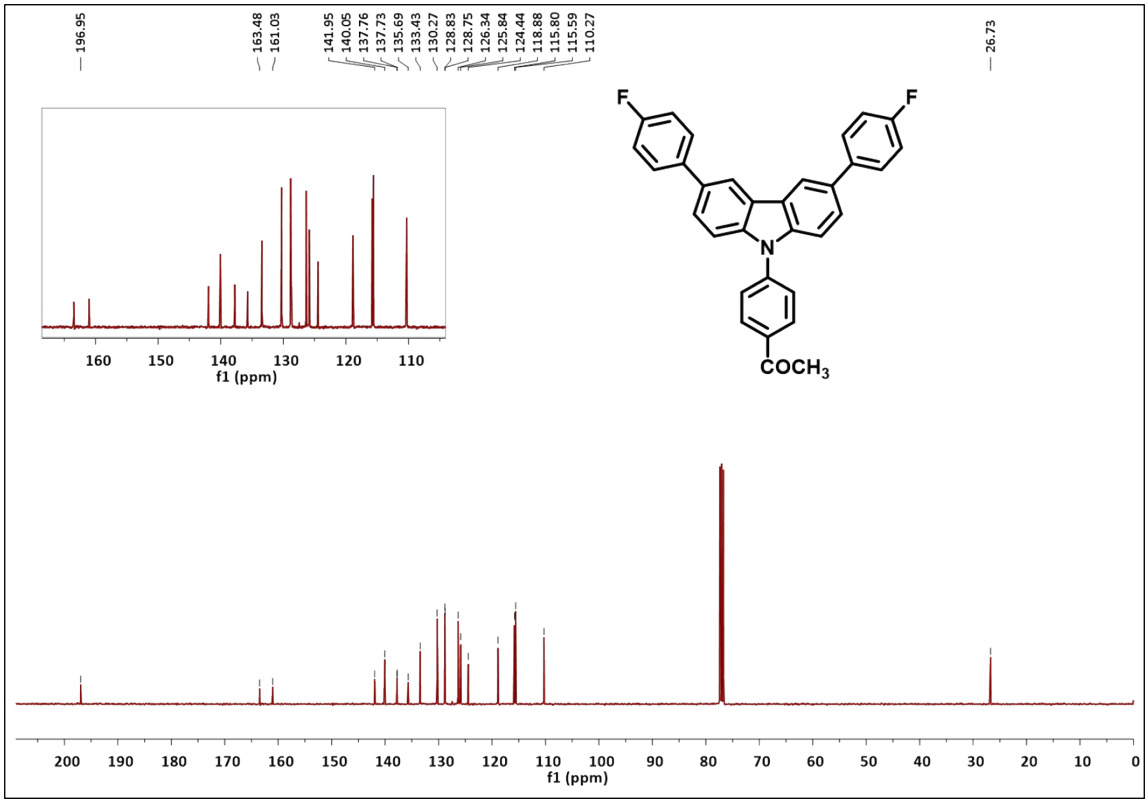

Figure SI 5: ^{1}H NMR & ^{19}F (top) and ^{13}C NMR (bottom) spectra of **DI-F-Acph** in $CDCl_3$

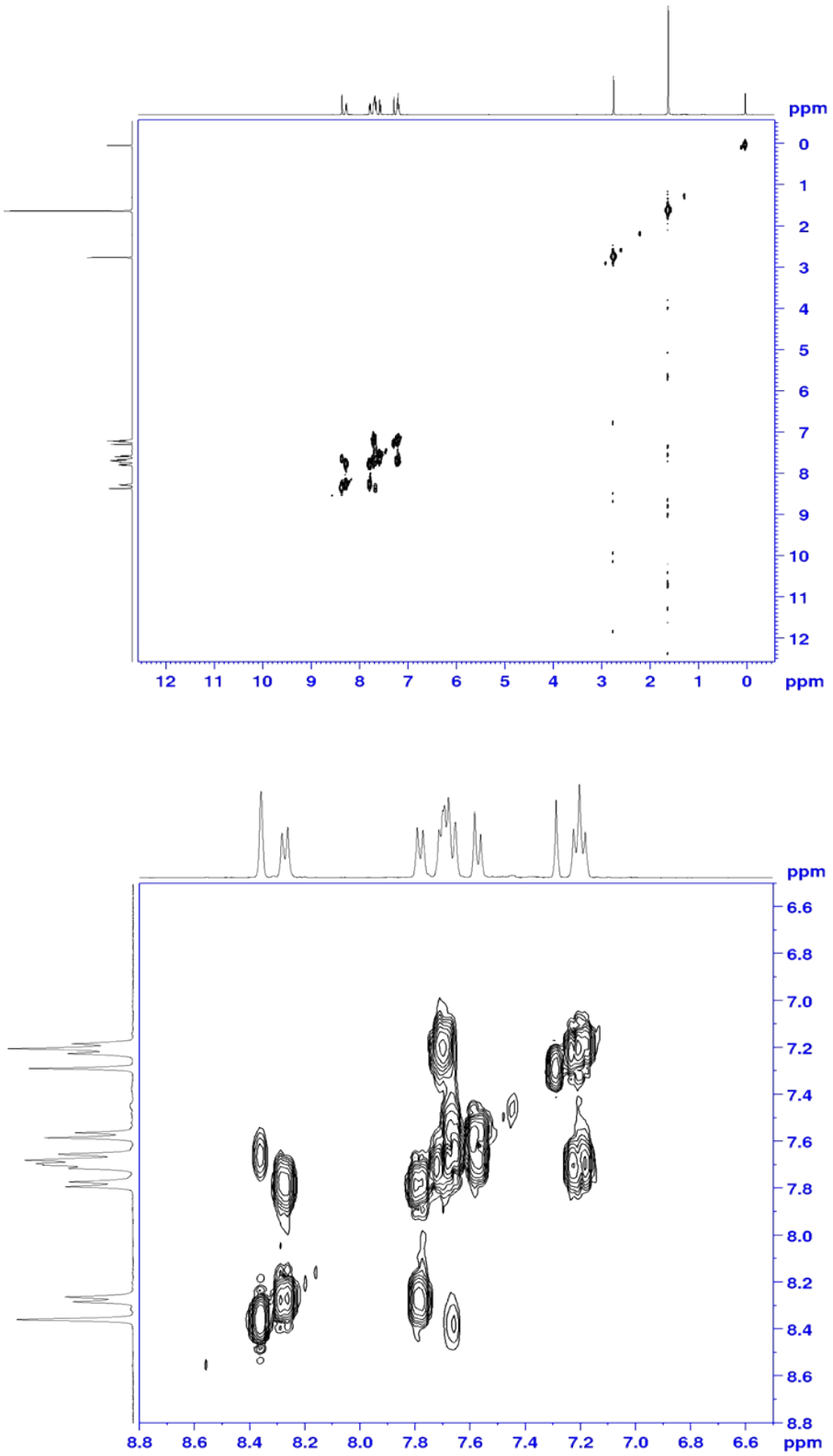

Figure SI 6: COSY spectrum of **DI-F-Acph** in $CDCl_3$. Top: Full spectrum and Bottom: Aromatic region

(ii) By mass spectrometry

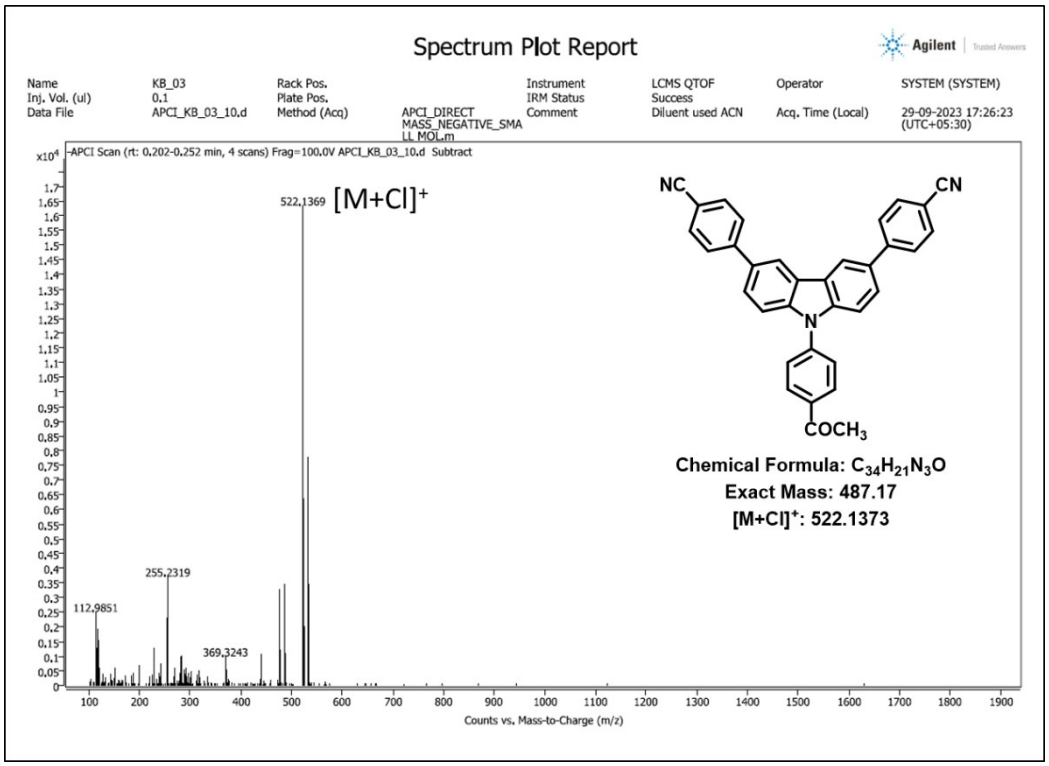

Figure SI 7: HRMS spectrum of compound **DI-CN-Acph**

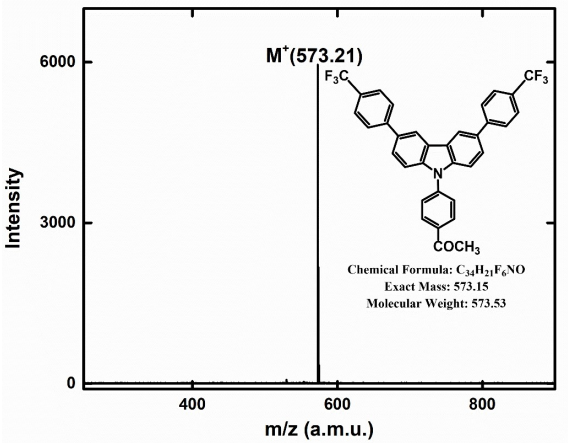

Figure SI 8: MALDI-TOF spectrum of compound **DI-CF_3-Acph**

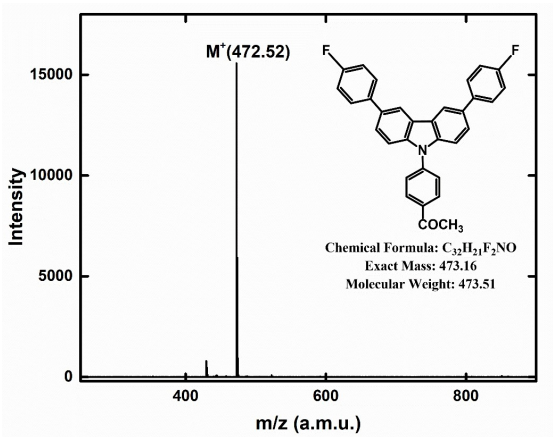

Figure SI 9: MALDI-TOF spectrum of compound **DI-F-Acph**

(iii) By FTIR spectroscopy

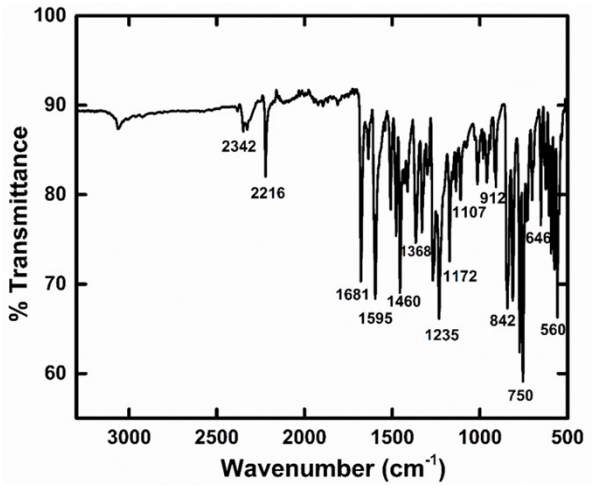

Figure SI 10: IR spectrum of compound **DI-CN-Acph**

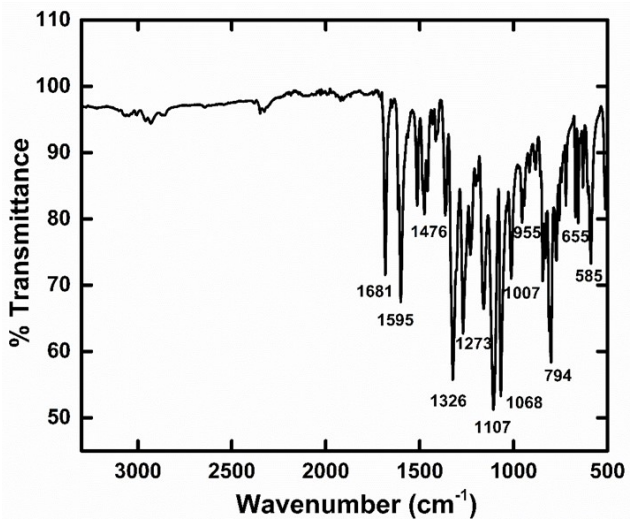

Figure SI 11: IR spectrum of compound **DI-CF_3-Acph**

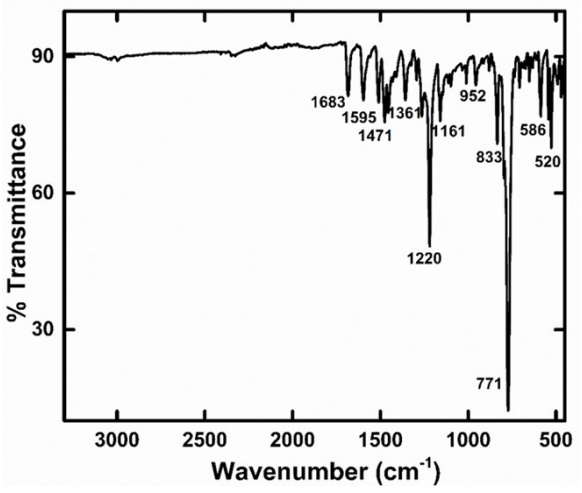

Figure SI 12: IR spectrum of compound **DI-F-Acph**

Photo-physical Studies:

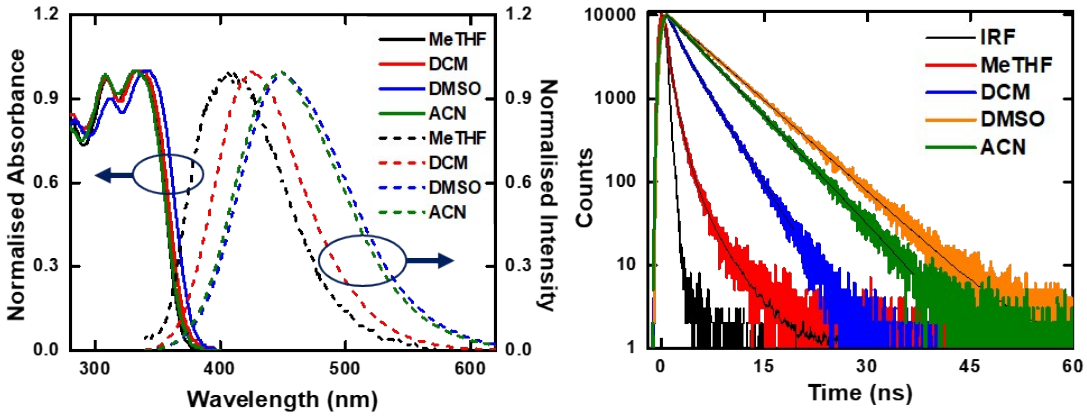

Figure SI 13: Absorption, emission & decay profiles of **DI-CN-Acph** in different solvents.

Table 1: Absorption & emission data of **DI-CN-Acph** in different solvents.

Solvent	λ_{abs} (nm) (log ε)	λ_{em} (nm)	Φ_f (%)	Stokes Shift (cm^{-1})
MeTHF	279 (4.87), 308 (4.94), 332 (4.95)	407	0.6	5550
DCM	280 (4.51), 308 (4.57), 335 (4.58)	445	5.2	7378
DMSO	283 (4.62), 312 (4.65), 341 (4.70)	470	29.2	8049
ACN	279 (4.56), 308 (4.66), 332 (4.66)	468	4.9	8753

Table 2: Lifetime data of **DI-CN-Acph** in different solvents.

Solvent	λ (nm)	Chi square	τ_1 (a_1) (ns)	τ_2 (a_2) (ns)	τ_3(a_3) (ns)	τ_{avg} (ns)
MeTHF	427	1.10	0.12±0.02 (64.6)	0.96±0.06 (29.9)	2.92± 0.16 (5.4)	0.78
DCM	453	1.2	1.07± 0.08 (17.4)	3.18± 0.03 (82.5)	-	2.81
DMSO	468	1.17	5.95± 0.01 (100)	-	-	5.95
ACN	473	1.11	5.05± 0.01 (100)	-	-	5.05

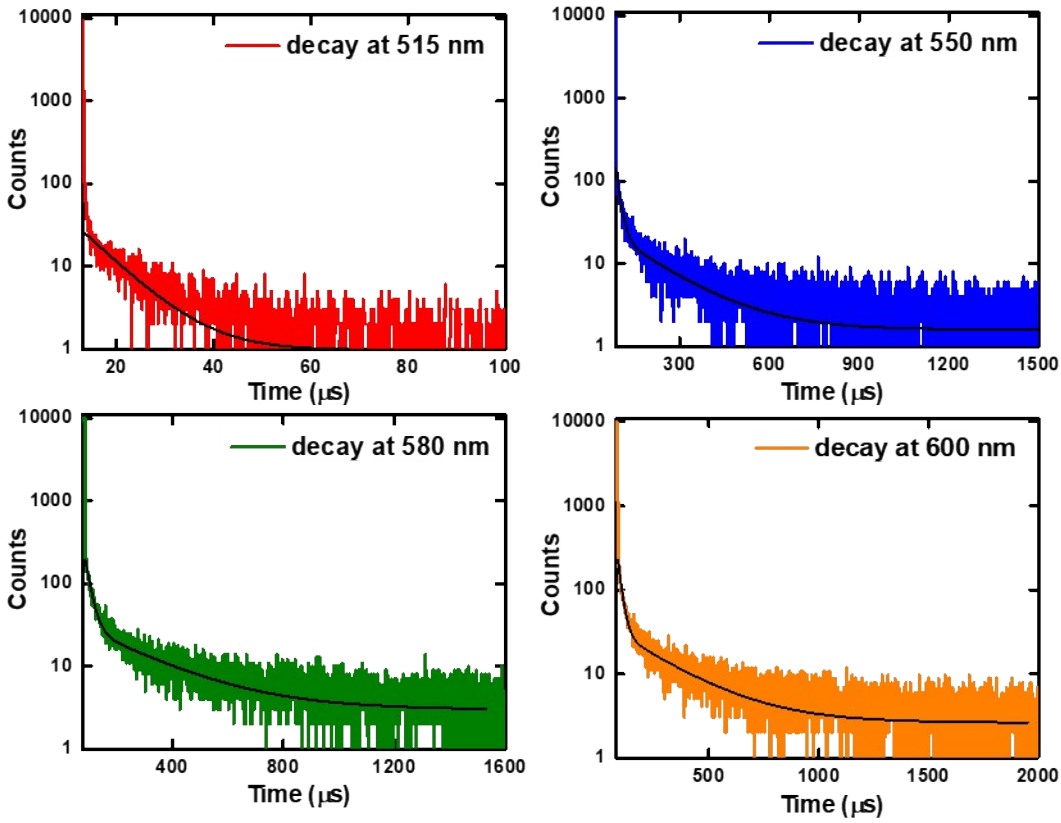

Figure SI 14: Emission decay profiles of **DI-CN-Acph** in powder at different wavelengths.

Table 3: Lifetime data of **DI-CN-Acph** in powder at different wavelengths.

λ (nm)	Chi square	τ_1 (a_1) (μs)	τ_2 (a_2) (μs)	τ_{avg} (μs)
515	1.12	7.7±1.2 (100)		7.7
550	1.09	14.2±2.1 (65.1)	170.7±24.2 (34.9)	21.0
580	1.18	19.4± 2.7 (60.7)	246.6±25.4 (39.3)	30.3
600	1.22	17.7±2.5 (65.8)	248.6±21.1 (34.2)	25.9

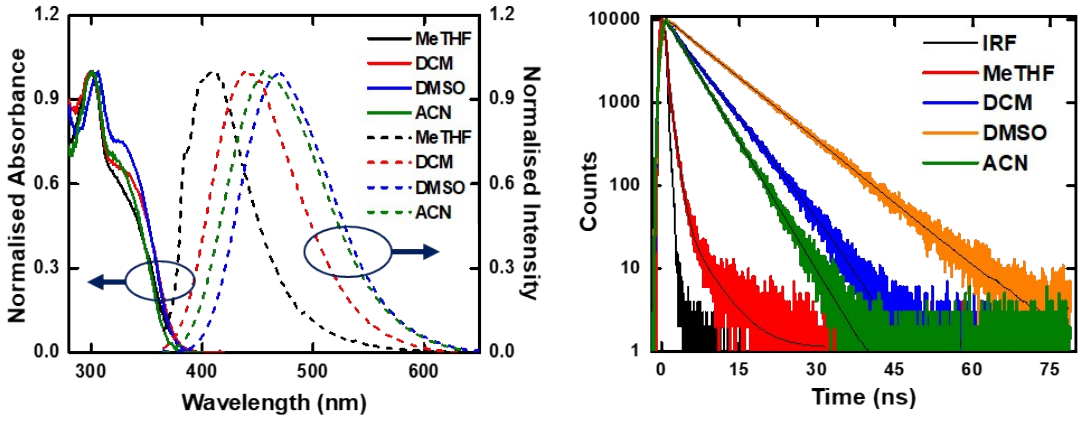

Figure SI 15: Absorption, emission & decay profiles of **DI-CF_3-Acph** in different solvents.

Table 4: Absorption & emission data of **DI-CF_3-Acph** in different solvents.

Solvent	λ_{abs} (nm) (log ε)	λ_{em} (nm)	Φ_f (%)	Stokes Shift (cm^{-1})
MeTHF	300 (4.61), 320 (4.46)	407	43.0	6678
DCM	300 (4.54), 320 (4.37)	455	27.3	9272
DMSO	305 (4.64), 325 (4.52)	468	37.1	9402
ACN	300 (4.51), 320 (4.11)	474	25.2	10153

Table 5: Lifetime data of **DI-CF_3-Acph** in different solvents.

Solvent	λ (nm)	Chi Square	τ_1 (a_1) (ns)	τ_2 (a_2) (ns)	τ_3 (a_3) (ns)	τ_{avg} (ns)
METHF	411	1.11	0.19±0.05 (54.5)	0.86±0.02 (43.3)	4.16±0.41 (2.2)	0.40
DCM	458	1.08	0.86±0.08(9.9)	5.38±0.02 (90.1)		3.55
DMSO	468	1.18	1.55± 0.18 (2.7)	8.70± 0.02 (97.3)		7.75
ACN	472	1.02	4.15± 0.01 (100)			4.15

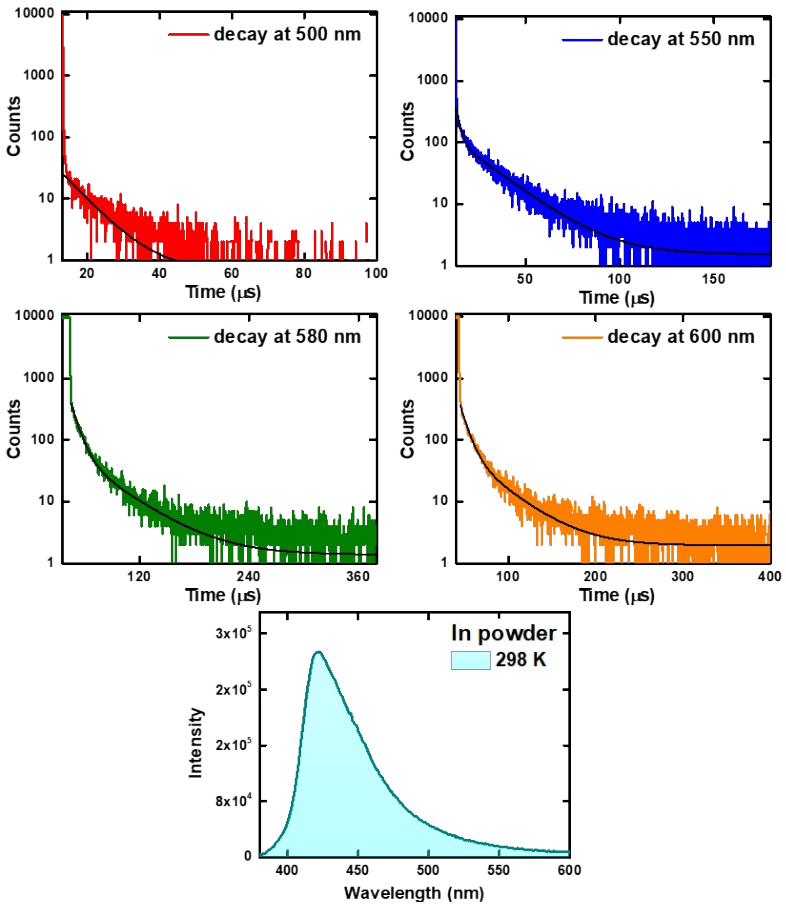

Figure SI 16: Emission & decay profiles of **DI-CF_3-Acph** in powder at different wavelengths.

Table 6: Lifetime data of **DI-CF_3-Acph** in powder at different wavelengths.

λ (nm)	Chi square	τ_1 (a_1) (μs)	τ_2 (a_2) (μs)	τ_{AVG} (μs)
500	1.06	7.0±0.9 (100)	-	7.0
550	1.13	1.9±0.5 (60.8)	18.9±0.7 (39.2)	3.0
580	1.06	8.2±0.6 (78.8)	41.4±9.9 (21.2)	9.8
600	1.19	8.3±1.3 (76.6)	37.6±3.9 (23.4)	10.0

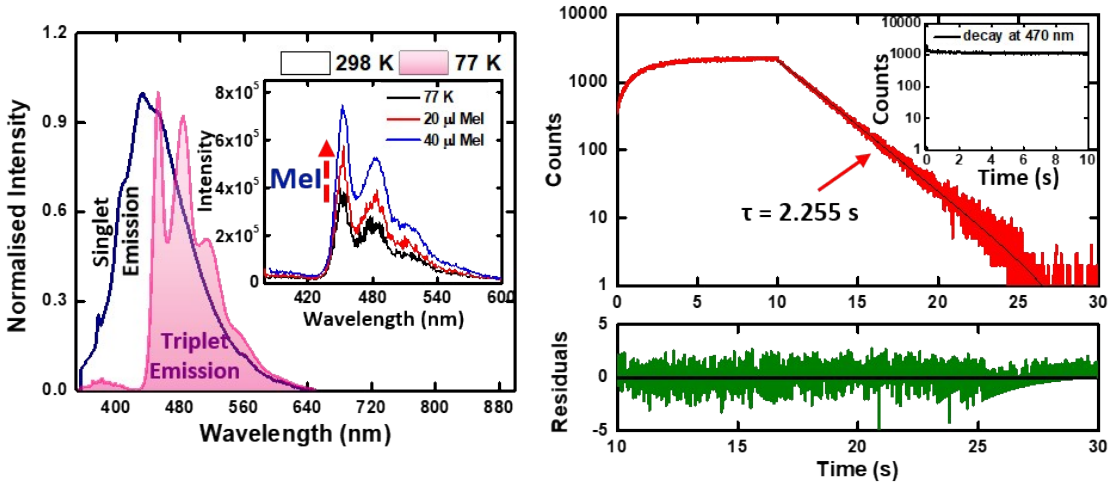

Figure SI 17: (Left) Emission of **DI-CF_3-Acph** in Me-THF at 298 K and 77 (inset emission at 77 K of **DI-CF_3-Acph** + MeI), & (Right) Kinetic scan at 77 K in MeTHF (inset decay profile) with excitation source ON for 10s.

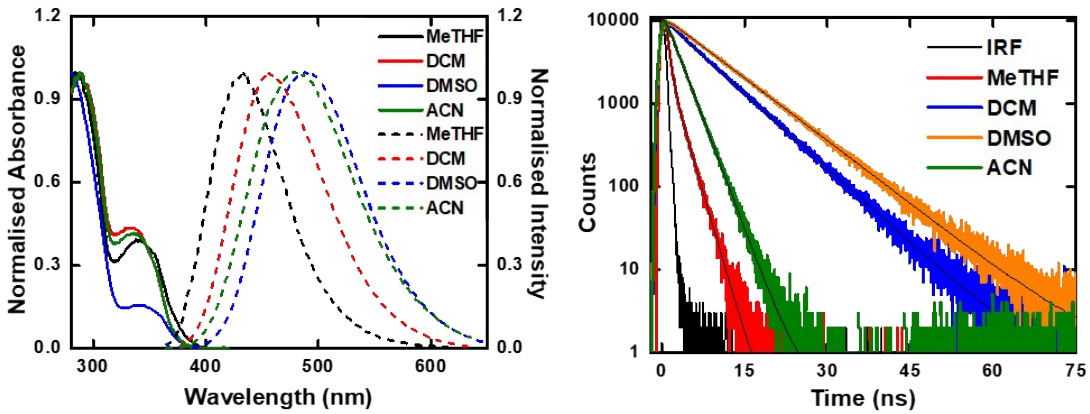

Figure SI 18: Absorption, emission & decay profiles of **DI-F-Acph** in different solvents.

Table 7: Absorption & emission data of **DI-F-Acph** in different solvents.

Solvent	λ_{abs} (nm) (log ε)	λ_{em} (nm)	Φ_f (%)	Stokes Shift (cm^{-1})
MeTHF	287 (4.61), 340 (4.24)	432	44.7	6263
DCM	287 (4.50), 334 (4.15)	471	31.5	8709
DMSO	287 (4.54), 334 (4.13)	489	12.6.	9490
ACN	287 (4.51), 336 (4.11)	496	25.7	9600

Table 8: Lifetime data of **DI-F-Acph** in different solvents.

Solvent	λ (nm)	Chi square	τ_1 (a_1) (ns)	τ_2 (a_2) (ns)	τ_{avg} (ns)
MeTHF	420	1.14	0.54±0.02 (58.4)	1.89± 0.02 (41.6)	0.77
DCM	475	1.02	1.14± 0.15 (3.1)	7.18± 0.01 (96.9)	6.18
DMSO	487	1.13	8.62± 0.01 (100)	-	8.62
ACN	495	1.03	2.43± 0.01 (100)	-	2.43

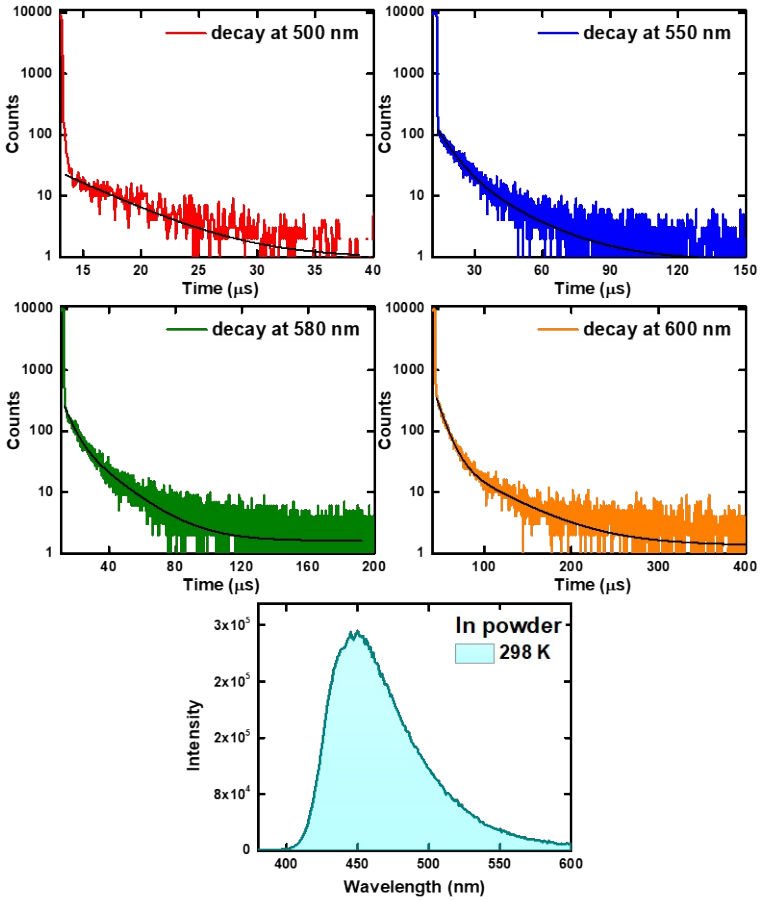

Figure SI 19: Emission & decay profiles of **DI-F-Acph** in powder at different wavelengths.

Table 9: Lifetime data of **DI-F-Acph** in powder at different wavelengths.

λ (nm)	Chi square	τ_1 (a_1) (μs)	τ_2 (a_2) (μs)	τ_3(A_3) (μs)
500	1.21	4.86±1.1 (100)	-	4.7
550	0.98	6.53±1.6 (64.5)	20.1±2.6 (35.5)	8.7
580	1.17	5.12±0.9 (39.4)	19.3±1.2 (60.6)	9.2
600	0.95	9.72±0.8 (85.0)	53.1±5.4 (14.9)	11.1

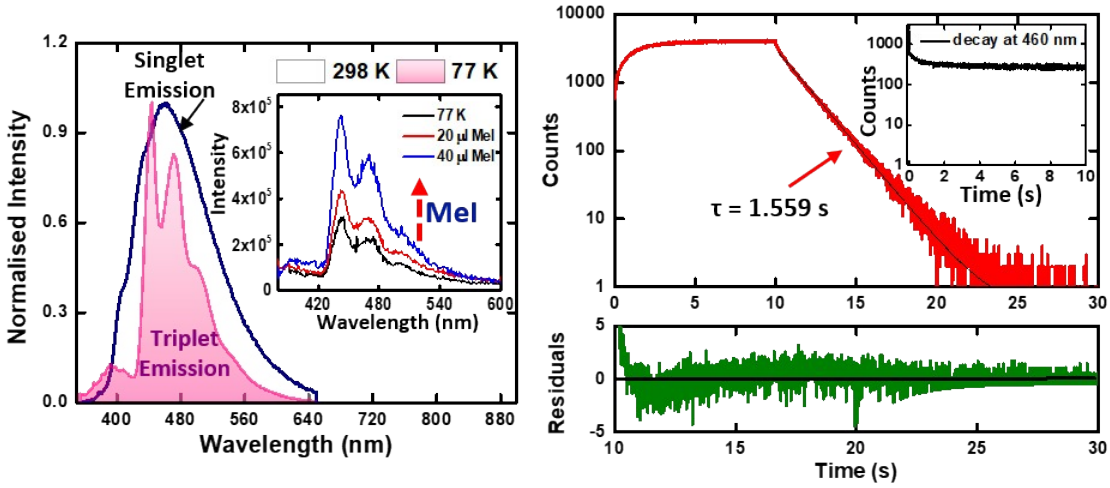

Figure SI 20: (Left) Emission of **DI-F-Acph** in Me-THF at 298 K and 77 (inset emission at 77 K of **DI-F-Acph** + MeI), & (Right) Kinetic scan at 77 K in MeTHF (inset decay profile) with excitation source ON for 10s.

Single Crystal studies:

The data were collected using Cu Kα radiation (λ = 1.54184 Å)from a single crystal at 298(2) K on an XtaLAB Synergy, Dualflex, HyPix four-circle diffractometer with a micro-focus sealed X-ray tube using a mirror as monochromator and a HyPix detector. All data were integrated with CrysAlis PRO and a multi-scan absorption correction using SCALE3 ABSPACK was applied. [3] The structure was solved by iterative methods using SHELXT and refined by full-matrix least-squares methods against F^2 by SHELXL-2017/1.[4] Hydrogen atoms were placed in idealized positions and were set riding on the respective parent atoms. All non-hydrogen atoms were refined with anisotropic thermal parameters. The structure was refined (weighted least squares refinement on F^2) to convergence. The crystal and structure refinement data are detailed in Table 10. All figures were drawn using ORTEP and Mercury. Crystallographic data (including structure factors) for the structures reported in this paper have been deposited with the Cambridge Crystallographic Data Centre.

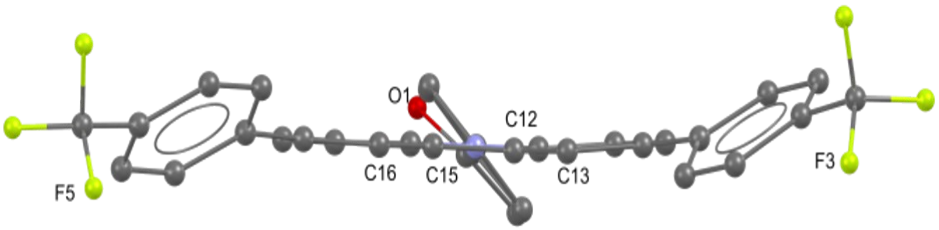

Molecule of DI-CF_3-Acph along b axis

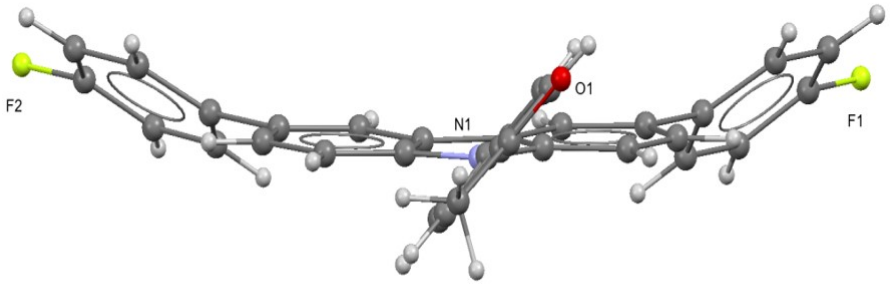

Molecule of DI-F-Acph along a axis

Figure SI 21: Crystal structures of **DI-CF_3-Acph & DI-F-Acph** along different axis**.**

Table 10: Crystallographic data for **DI-CF_3-Acph & DI-F-Acph**

Compound	DI-CF_3-Acph	DI-F-Acph
Empirical formula	$C_{34}H_{21}F_6NO$	$C_{32}H_{21}F_2NO$
Formula weight	573.52	473.50
Temperature [K]	298(2)	298(2)
Crystal system	orthorhombic	monoclinic
Space group (number)	$Pca2_1$ (29)	$P2_1/c$ (14)
a [Å]	27.071(9)	14.54460(10)
b [Å]	13.5223(6)	21.9876(5)
c [Å]	7.5005(4)	7.50510(10)
α [Å]	90	90
β [Å]	90	101.3830(10)
γ [Å]	90	90
Volume [Å^3]	2745.6(10)	2352.93(6)
Z	4	4
ρ_{calc} [g/cm^3]	1.387	1.337
μ [mm^{-1}]	0.952	0.742
F(000)	1176	984
Crystal size [mm^3]	0.150×0.050×0.020	0.100×0.050×0.010
Crystal colour	colourless	colourless
Crystal shape	plate	plate
Radiation	Cu K_α (λ=1.54184 Å)	Cu K_α (λ=1.54184 Å)
2Θ range [°]	6.53 to 155.70 (0.79 Å)	6.20 to 174.11 (0.77 Å)
Index ranges	-34 ≤ h ≤ 34 -17 ≤ k ≤ 16 -9 ≤ l ≤ 7	-18 ≤ h ≤ 18 -25 ≤ k ≤ 27 -9 ≤ l ≤ 9
Reflections collected	26690	91708
Independent reflections	4748 R_{int} = 0.0784 R_{sigma} = 0.0520	5049 R_{int} = 0.1481 R_{sigma} = 0.0432
Completeness to θ = 67.684°	100.0 %	99.9 %
Data / Restraints / Parameters	4748/13/399	5049/0/326
Goodness-of-fit on F^2	1.301	1.031
Final R indexes [I≥2σ(I)]	R_1 = 0.0651 wR_2 = 0.2021	R_1 = 0.0791 wR_2 = 0.2417
Final R indexes [all data]	R_1 = 0.0874 wR_2 = 0.2847	R_1 = 0.0936 wR_2 = 0.2643
Largest peak/hole [eÅ^3]	0.47/-0.48	0.35/-0.26
CCDC number	2299335	2299336

Table 11. Bond lengths and angles for **DI-CF_3-Acph**

	Length[Å]/Angle[°]
C1–C2	1.513(6)
C1–F1	1.313(10)
C1–F2A	1.38(3)
C1–F2B	1.295(12)
C1–F3	1.334(10)
C2–C3	1.382(7)
C2–C7	1.381(8)
C3–C4	1.384(6)
C4–C5	1.382(6)
C5–C6	1.388(6)
C5–C8	1.493(5)
C6–C7	1.389(6)
C8–C13	1.374(6)
C8–C9	1.419(5)
C9–C10	1.377(6)
C10–C11	1.385(6)
C11–C12	1.411(5)
C11–N1	1.393(5)
C12–C13	1.399(5)
C12–C15	1.433(5)
C14–C15	1.413(5)
C14–C19	1.384(5)
C14–N1	1.401(5)
C15–C16	1.388(6)
C16–C17	1.382(6)
C17–C18	1.415(6)
C17–C20	1.486(5)
C18–C19	1.375(6)
C20–C21	1.389(6)
C20–C25	1.400(6)
C21–C22	1.373(7)
C22–C23	1.387(8)
C23–C24	1.376(9)
C23–C26	1.511(8)
C24–C25	1.380(7)
C26–F4	1.296(10)
C26–F5A	1.36(4)
C26–F5B	1.287(16)
C26–F6	1.338(13)
C27–C28	1.395(6)
C27–C32	1.391(7)
C27–N1	1.429(5)
C28–C29	1.382(6)
C29–C30	1.402(7)
C30–C31	1.382(7)
C30–C33	1.508(5)
C31–C32	1.380(6)

C33–C34	1.469(8)
C33–O1	1.226(8)
Bond angles	
F1–C1–C2	112.7(6)
F2A–C1–C2	114.9(14)
F2B–C1–C2	111.0(7)
F3–C1–C2	112.4(6)
F2B–C1–F1	112.8(14)
F1–C1–F2A	89(3)
F3–C1–F2A	119(2)
F1–C1–F3	106.3(6)
F2B–C1–F3	101.1(12)
C3–C2–C1	119.4(5)
C7–C2–C1	120.3(5)
C7–C2–C3	120.3(4)
C2–C3–C4	119.9(4)
C5–C4–C3	120.9(4)
C4–C5–C6	118.3(4)
C4–C5–C8	120.7(4)
C6–C5–C8	121.0(4)
C5–C6–C7	121.5(4)
C2–C7–C6	119.0(5)
C13–C8–C5	119.8(3)
C9–C8–C5	121.2(4)
C13–C8–C9	118.9(3)
C10–C9–C8	122.9(4)
C9–C10–C11	117.3(4)
C10–C11–C12	121.3(4)
N1–C11–C12	108.7(3)
C10–C11–N1	129.8(4)
C13–C12–C11	120.0(4)
C11–C12–C15	107.7(3)
C13–C12–C15	132.3(4)
C8–C13–C12	119.6(4)
C19–C14–C15	120.4(4)
N1–C14–C15	109.2(4)
C19–C14–N1	130.3(4)
C14–C15–C12	106.4(3)
C16–C15–C12	132.9(4)
C16–C15–C14	120.7(4)
C17–C16–C15	119.5(4)
C16–C17–C18	118.5(4)
C16–C17–C20	120.1(4)
C18–C17–C20	121.3(4)
C19–C18–C17	122.8(4)
C18–C19–C14	117.9(4)
C21–C20–C17	120.9(4)
C25–C20–C17	121.0(4)
C21–C20–C25	118.1(4)
C22–C21–C20	121.1(4)

C21–C22–C23	119.8(5)
C24–C23–C22	120.5(5)
C22–C23–C26	119.8(6)
C24–C23–C26	119.7(6)
C23–C24–C25	119.4(5)
C24–C25–C20	121.1(5)
F4–C26–C23	113.2(6)
F5A–C26–C23	106.8(14)
F5B–C26–C23	115.4(9)
F6–C26–C23	111.5(8)
F5B–C26–F4	101.9(17)
F4–C26–F5A	134(3)
F6–C26–F5A	84(3)
F4–C26–F6	101.6(8)
F5B–C26–F6	112.1(14)
C32–C27–C28	119.8(4)
C28–C27–N1	120.2(4)
C32–C27–N1	120.0(4)
C29–C28–C27	119.6(4)
C28–C29–C30	121.4(4)
C31–C30–C29	117.5(4)
C29–C30–C33	123.1(4)
C31–C30–C33	119.3(4)
C32–C31–C30	122.2(4)
C31–C32–C27	119.4(4)
C34–C33–C30	121.0(5)
O1–C33–C30	119.0(5)
O1–C33–C34	119.9(5)
C11–N1–C14	108.0(3)
C11–N1–C27	125.9(3)
C14–N1–C27	126.1(3)

Table 12. Bond lengths and angles for **DI-F-Acph.**

No	**Length[Å]/Angle[°]**
C1– C2	1.398(5)
C2– C3	1.499(4)
C2– O1	1.291(5)
C3– C4	1.389(4)
C3– C8	1.397(4)
C4– C5	1.381(3)
C5– C6	1.389(3)
C6– C7	1.393(3)
C6– N1	1.419(3)
C7– C8	1.378(4)
C9– C10	1.403(3)
C9– C23	1.387(3)
C9– N1	1.407(3)
C10– C11	1.446(3)

C10– C26	1.393(3)
C11– C12	1.402(3)
C11– C16	1.390(3)
C12– C13	1.403(4)
C12– N1	1.399(3)
C13– C14	1.376(3)
C14– C15	1.404(4)
C15– C16	1.392(3)
C15– C17	1.485(3)
C17– C18	1.384(4)
C17– C22	1.395(4)
C18– C19	1.386(4)
C19– C20	1.346(4)
C20– C21	1.366(5)
C20– F1	1.368(3)
C21– C22	1.383(5)
C23– C24	1.387(3)
C24– C25	1.400(3)
C25– C26	1.391(3)
C25– C27	1.488(3)
C27– C28	1.396(3)
C27– C32	1.392(4)
C28– C29	1.386(4)
C29– C30	1.363(4)
C30– C31	1.368(4)
C30– F2	1.356(3)
C31– C32	1.384(4)
Bond angles	
O1– C2– C1	121.4(4)
O1– C2– C3	119.5(3)
C1– C2– C3	119.0(4)
C4– C3– C2	123.0(3)
C8– C3– C2	119.1(3)
C4– C3– C8	117.9(2)
C5– C4– C3	121.6(2)
C4– C5– C6	119.8(2)
C5– C6– C7	119.1(2)
C5– C6– N1	120.5(2)
C7– C6– N1	120.4(2)
C8– C7– C6	120.5(2)
C7– C8– C3	120.9(2)
C23– C9– C10	120.7(2)
C23– C9– N1	130.7(2)
C10– C9– N1	108.5(2)
C26– C10– C11	132.2(2)
C9– C10– C11	107.4(2)
C26– C10– C9	120.2(2)
C16– C11– C10	132.8(2)
C12– C11– C10	106.7(2)
C16– C11– C12	120.5(2)

N1– C12– C11	109.3(2)
N1– C12– C13	130.0(2)
C11– C12– C13	120.7(2)
C14– C13– C12	117.6(2)
C13– C14– C15	122.8(2)
C16– C15– C14	118.9(2)
C16– C15– C17	121.0(2)
C14– C15– C17	120.1(2)
C11– C16– C15	119.5(2)
C18– C17– C15	121.3(2)
C22– C17– C15	121.5(2)
C18– C17– C22	117.3(2)
C17– C18– C19	121.2(2)
C20– C19– C18	119.3(3)
C19– C20– C21	122.3(3)
C19– C20– F1	118.6(3)
C21– C20– F1	119.1(3)
C20– C21– C22	118.3(3)
C21– C22– C17	121.6(3)
C9– C23– C24	118.1(2)
C23– C24– C25	122.4(2)
C26– C25– C24	118.7(2)
C26– C25– C27	120.9(2)
C24– C25– C27	120.4(2)
C25– C26– C10	119.9(2)
C32– C27– C25	121.3(2)
C28– C27– C25	121.2(2)
C32– C27– C28	117.5(2)
C29– C28– C27	121.4(3)
C30– C29– C28	118.7(3)
F2– C30– C29	119.3(3)
F2– C30– C31	118.3(3)
C29– C30– C31	122.4(3)
C30– C31– C32	118.5(3)
C31– C32– C27	121.6(2)
C12– N1– C6	125.71(19)
C9– N1– C6	125.54(19)
C12– N1– C9	108.01(19)

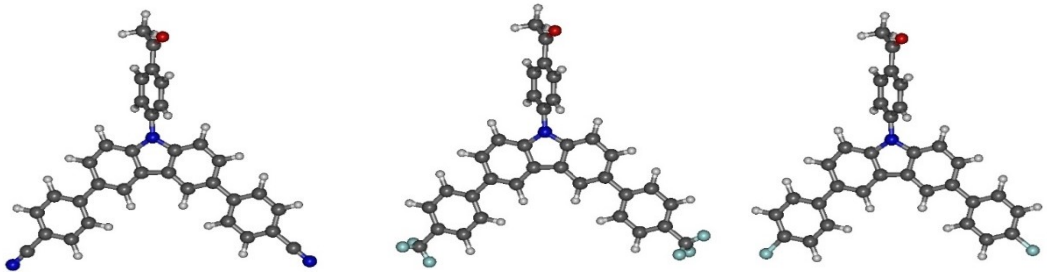

Figure SI 22: Optimized geometries of **DI-CN-Acph, DI-CF_3-Acph & DI-F-Acph.**

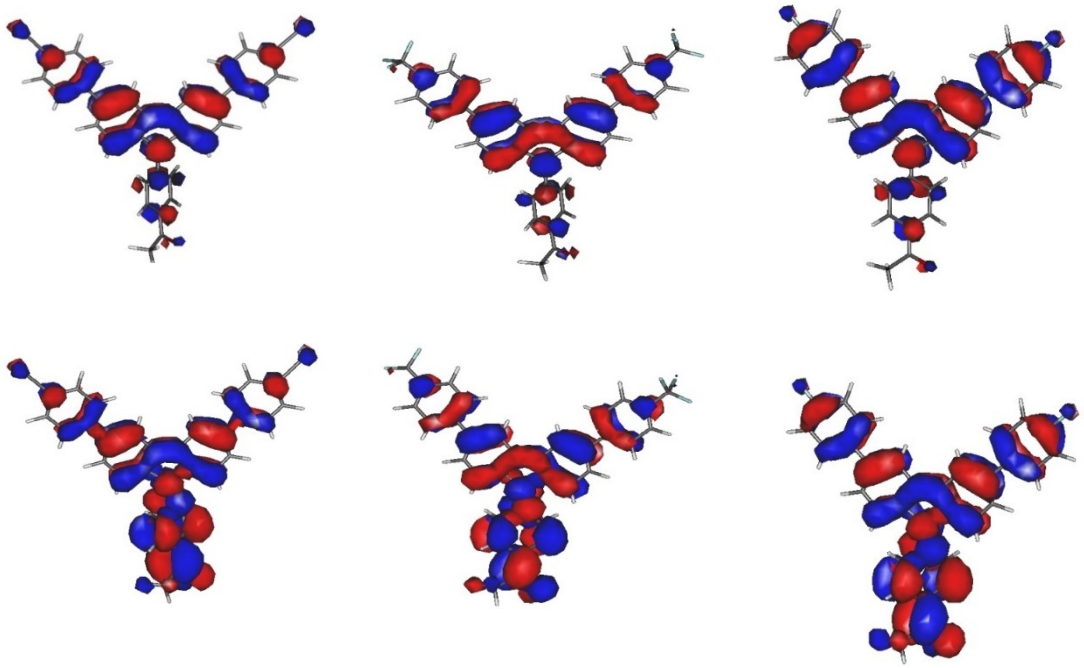

Figure SI 23: Calculated frontier molecular orbitals of **DI-CN-Acph, DI-CF_3-Acph & DI-F-Acph.**

References:

1 Ling, K., Shi, H., Wang, H., Fu, L., Lv, A., Huang, K., Ye, W., Gu, M., Ma, C., Yao, X. and Jia, W., *Advanced Optical Materials*, 2019, **7(24)**, p.1901076.
2 Agarwal, N., Nayak, P.K., Ali, F., Patankar, M.P., Narasimhan, K.L. and Periasamy, N., *Synthetic metals*, 2011, **161(5-6)**, pp.466-473.
3 Rigaku Oxford Diffraction (2015). CrysAlis PRO. Rigaku Oxford Diffraction, Yarnton, England.
4 G. M. Sheldrick, *Acta Cryst.*2015, **C71**, 3–8.